Resource

Cell

Integrative Clinical Genomics of Advanced Prostate Cancer

Graphical Abstract

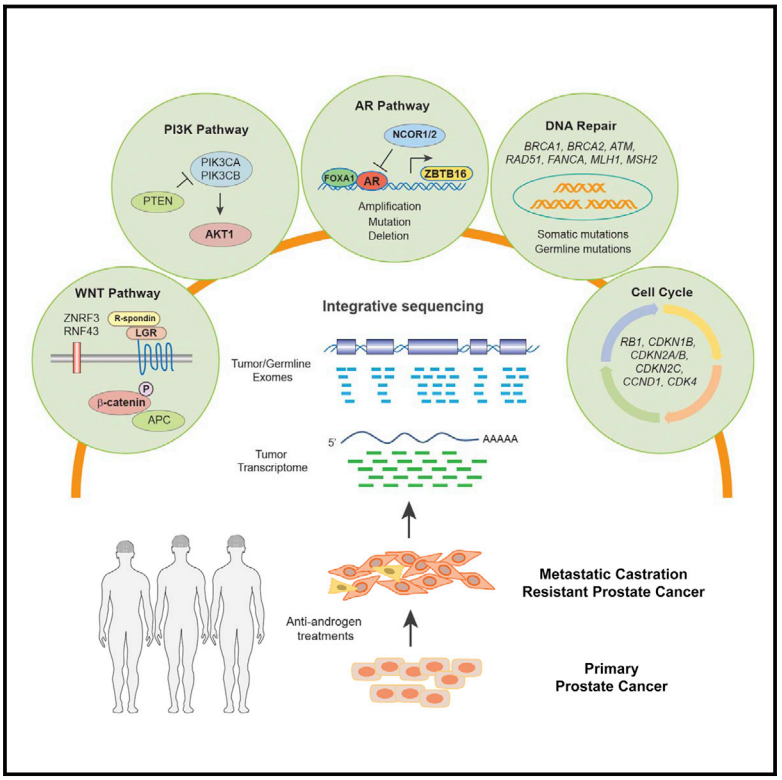

Highlights

- A multi-institutional integrative clinical sequencing of mCRPC
- Approximately 90% of mCRPC harbor clinically actionable molecular alterations
- mCRPC harbors genomic alterations in *PIK3CA/B*, *RSPO*, *RAF*, *APC*, β-catenin, and *ZBTB16*
- 23% of mCRPC harbor DNA repair pathway aberrations, and 8% harbor germline findings

Authors

Dan Robinson, Eliezer M. Van Allen, ..., Charles L. Sawyers, Arul M. Chinnaiyan

Correspondence

sawyersc@mskcc.org (C.L.S.), arul@umich.edu (A.M.C.)

In Brief

A multi-institutional integrative clinical sequencing analysis reveals that the majority of affected individuals with metastatic castration-resistant prostate cancer harbor clinically actionable molecular alterations, highlighting the need for genetic counseling to inform precision medicine in affected individuals with advanced prostate cancer.

Robinson et al., 2015, Cell *161*, 1215–1228
May 21, 2015
http://dx.doi.org/10.1016/j.cell.2015.05.001

CellPress

Resource

Cell

Integrative Clinical Genomics of Advanced Prostate Cancer

Dan Robinson,[1,2,43] Eliezer M. Van Allen,[3,4,43] Yi-Mi Wu,[1,2] Nikolaus Schultz,[5,40] Robert J. Lonigro,[1] Juan-Miguel Mosquera,[6,7,8,38] Bruce Montgomery,[9,10] Mary-Ellen Taplin,[3] Colin C. Pritchard,[26] Gerhardt Attard,[11,12] Himisha Beltran,[7,8,13,38] Wassim Abida,[14,20] Robert K. Bradley,[9] Jake Vinson,[15] Xuhong Cao,[1,42] Pankaj Vats,[1] Lakshmi P. Kunju,[1,2,17] Maha Hussain,[16,17,18] Felix Y. Feng,[1,17,19] Scott A. Tomlins,[1,2,17,18] Kathleen A. Cooney,[16,17,18] David C. Smith,[16,17,18] Christine Brennan,[1] Javed Siddiqui,[1] Rohit Mehra,[1,2] Yu Chen,[13,14,20] Dana E. Rathkopf,[13,20] Michael J. Morris,[13,20] Stephen B. Solomon,[21] Jeremy C. Durack,[21] Victor E. Reuter,[22] Anuradha Gopalan,[22] Jianjiong Gao,[40] Massimo Loda,[3,4,23,39] Rosina T. Lis,[3,23] Michaela Bowden,[3,23,39] Stephen P. Balk,[24] Glenn Gaviola,[25] Carrie Sougnez,[4] Manaswi Gupta,[4] Evan Y. Yu,[10] Elahe A. Mostaghel,[9,10] Heather H. Cheng,[9,10] Hyojeong Mulcahy,[27] Lawrence D. True,[28] Stephen R. Plymate,[10] Heidi Dvinge,[9] Roberta Ferraldeschi,[11,12] Penny Flohr,[11,12] Susana Miranda,[11,12] Zafeiris Zafeiriou,[11,12] Nina Tunariu,[11,12] Joaquin Mateo,[11,12] Raquel Perez-Lopez,[11,12] Francesca Demichelis,[7,29] Brian D. Robinson,[6,7,8,38] Marc Schiffman,[7,31,38] David M. Nanus,[7,8,13,38] Scott T. Tagawa,[7,8,13,38] Alexandros Sigaras,[7,30,32] Kenneth W. Eng,[7,30,32] Olivier Elemento,[30] Andrea Sboner,[6,7,30,38] Elisabeth I. Heath,[33,34] Howard I. Scher,[13,20] Kenneth J. Pienta,[35] Philip Kantoff,[3,44] Johann S. de Bono,[11,12,44] Mark A. Rubin,[6,7,8,38,44] Peter S. Nelson,[10,36,37,38,44] Levi A. Garraway,[3,4,44] Charles L. Sawyers,[14,41,44,*] and Arul M. Chinnaiyan[1,2,17,18,42,44,*]

[1]Michigan Center for Translational Pathology, University of Michigan Medical School, Ann Arbor, MI 48109, USA
[2]Department of Pathology, University of Michigan Medical School, Ann Arbor, MI 48109, USA
[3]Department of Medical Oncology, Dana-Farber Cancer Institute, Boston, MA 02215, USA
[4]Broad Institute of Massachusetts Institute of Technology and Harvard, Cambridge, MA 02142, USA
[5]Department of Epidemiology and Biostatistics, Memorial Sloan Kettering Cancer Center, New York, NY 10065, USA
[6]Department of Pathology and Laboratory Medicine, Weill Medical College of Cornell University, New York, NY 10021, USA
[7]Institute for Precision Medicine, Weill Medical College of Cornell University, New York, NY 10021, USA
[8]New York Presbyterian Hospital, New York, NY 10021, USA
[9]Computational Biology Program, Public Health Sciences Division and Basic Science Division, Fred Hutchinson Cancer Center, University of Washington, Seattle, WA 98109, USA
[10]Department of Medicine and VAPSHCS, University of Washington, Seattle, WA 98109, USA
[11]Cancer Biomarkers Team, Division of Clinical Studies, The Institute of Cancer Research, London SM2 5NG, UK
[12]Prostate Cancer Targeted Therapy Group and Drug Development Unit, The Royal Marsden NHS Foundation Trust, London SM2 5NG, UK
[13]Department of Medicine, Weill Medical College of Cornell University, New York, NY 10021, USA
[14]Human Oncology and Pathogenesis Program, Memorial Sloan Kettering Cancer Center, New York, NY 10065, USA
[15]Prostate Cancer Clinical Trials Consortium, Memorial Sloan Kettering Cancer Center, New York, NY 10065, USA
[16]Department of Internal Medicine, Division of Hematology Oncology, University of Michigan Medical School, Ann Arbor, MI 48109, USA
[17]Comprehensive Cancer Center, University of Michigan Medical School, Ann Arbor, MI 48109, USA
[18]Department of Urology, University of Michigan Medical School, Ann Arbor, MI 48109, USA
[19]Department of Radiation Oncology, University of Michigan Medical School, Ann Arbor, MI 48109, USA
[20]Genitourinary Oncology Service, Department of Medicine, Sidney Kimmel Center for Prostate and Urologic Cancers, Memorial Sloan Kettering Cancer Center, New York, NY 10065, USA
[21]Interventional Radiology, Department of Radiology Service, Memorial Sloan Kettering Cancer Center, New York, NY 10065, USA
[22]Department of Pathology, Memorial Sloan Kettering Cancer Center, New York, NY 10065, USA
[23]Center for Molecular Oncologic Pathology, Dana-Farber Cancer Institute, Boston, MA 02215, USA
[24]Division of Hematology-Oncology, Department of Medicine, Beth Israel Deaconess Cancer Center, Beth Israel Deaconess Medical Center, Harvard Medical School, Boston, MA 02215, USA
[25]Department of Musculoskeletal Radiology, Brigham and Women's Hospital, Boston, MA 02115, USA
[26]Department of Laboratory Medicine, University of Washington, Seattle, WA 98195, USA
[27]Department of Radiology, University of Washington, Seattle, WA 98109, USA
[28]Department of Pathology, University of Washington Medical Center, Seattle, WA 98109, USA
[29]Laboratory of Computational Oncology, CIBIO, Centre for Integrative Biology, University of Trento, 38123 Mattarello TN, Italy
[30]Institute for Computational Biomedicine, Department of Physiology and Biophysics, Weill Medical College of Cornell University, New York, NY 10021, USA
[31]Division of Interventional Radiology, Department of Radiology, New York-Presbyterian Hospital/Weill Cornell Medical Center, New York, NY 10021, USA
[32]Department of Physiology & Biophysics, Weill Medical College of Cornell University, New York, NY 10021, USA
[33]Department of Oncology, Wayne State University School of Medicine, Detroit, MI 48201, USA
[34]Molecular Therapeutics Program, Barbara Ann Karmanos Cancer Institute, Detroit, MI 48201, USA
[35]The James Buchanan Brady Urological Institute and Department of Urology, Johns Hopkins School of Medicine, Baltimore, MD 21205, USA
[36]Division of Human Biology, Fred Hutchinson Cancer Research Center, Seattle, WA 98109, USA
[37]Division of Clinical Research, Fred Hutchinson Cancer Research Center, Seattle, WA 98109, USA
[38]Meyer Cancer, Weill Medical College of Cornell University, New York, NY 10021, USA

[39]Department of Pathology, Brigham & Women's Hospital, Boston, MA 02115, USA
[40]Marie-Josée and Henry R. Kravis Center for Molecular Oncology, Memorial Sloan Kettering Cancer Center, New York, NY 10065, USA
[41]Howard Hughes Medical Institute, Memorial Sloan Kettering Cancer Center, New York, NY 10065, USA
[42]Howard Hughes Medical Institute, University of Michigan, Ann Arbor, MI 48109, USA
[43]Co-first author
[44]Co-senior author
*Correspondence: sawyersc@mskcc.org (C.L.S.), arul@umich.edu (A.M.C.)
http://dx.doi.org/10.1016/j.cell.2015.05.001

SUMMARY

Toward development of a precision medicine framework for metastatic, castration-resistant prostate cancer (mCRPC), we established a multi-institutional clinical sequencing infrastructure to conduct prospective whole-exome and transcriptome sequencing of bone or soft tissue tumor biopsies from a cohort of 150 mCRPC affected individuals. Aberrations of *AR*, ETS genes, *TP53*, and *PTEN* were frequent (40%–60% of cases), with *TP53* and *AR* alterations enriched in mCRPC compared to primary prostate cancer. We identified new genomic alterations in *PIK3CA/B*, R-spondin, *BRAF/RAF1*, *APC*, β-catenin, and *ZBTB16/PLZF*. Moreover, aberrations of *BRCA2*, *BRCA1*, and *ATM* were observed at substantially higher frequencies (19.3% overall) compared to those in primary prostate cancers. 89% of affected individuals harbored a clinically actionable aberration, including 62.7% with aberrations in AR, 65% in other cancer-related genes, and 8% with actionable pathogenic germline alterations. This cohort study provides clinically actionable information that could impact treatment decisions for these affected individuals.

INTRODUCTION

Prostate cancer is among the most common adult malignancies, with an estimated 220,000 American men diagnosed yearly (American Cancer Society, 2015). Some men will develop metastatic prostate cancer and receive primary androgen deprivation therapy (ADT). However, nearly all men with metastatic prostate cancer develop resistance to primary ADT, a state known as metastatic castration-resistant prostate cancer (mCRPC). Multiple "second generation" ADT treatments, like abiraterone acetate (de Bono et al., 2011; Ryan et al., 2013) and enzalutamide (Beer et al., 2014; Scher et al., 2012), have emerged for mCRPC affected individuals; however, nearly all affected individuals will also develop resistance to these agents. In the U.S., an estimated 30,000 men die of prostate cancer yearly.

Multiple studies have identified recurrent somatic mutations, copy number alterations, and oncogenic structural DNA rearrangements (chromoplexy) in primary prostate cancer (Baca et al., 2013; Barbieri et al., 2012; Berger et al., 2011; Cooper et al., 2015; Pflueger et al., 2011; Taylor et al., 2010; Tomlins et al., 2007; Wang et al., 2011). These include point mutations in *SPOP*, *FOXA1*, and *TP53*; copy number alterations involving *MYC*, *RB1*, *PTEN*, and *CHD1*; and E26 transformation-specific (ETS) fusions, among other biologically relevant genes. Although certain primary prostate cancer alterations or signatures have prognostic clinical significance (Hieronymus et al., 2014; Lalonde et al., 2014), the therapeutic impact of primary prostate cancer genomic events has not yet been realized.

Genomic studies of metastatic prostate cancers demonstrated additional alterations in *AR* (Taplin et al., 1995) and in the androgen signaling pathway (Beltran et al., 2013; Grasso et al., 2012; Gundem et al., 2015; Hong et al., 2015), although these studies were performed predominantly using autopsy samples or preclinical models with limited cohort sizes. Prospective genomic characterization of fresh biopsy samples from living mCRPC affected individuals has been limited due to challenges in obtaining adequate tumor tissue, especially from bone biopsies (Mehra et al., 2011; Van Allen et al., 2014a), which is the most common site of metastatic disease. Thus, the landscape of genomic alterations in mCRPC disease remains incompletely characterized. Moreover, the low frequency of actionable genomic alterations in primary prostate cancer has limited the inclusion of mCRPC among cohorts wherein precision cancer medicine approaches have been piloted to guide treatment or clinical trial enrollment.

We conducted a systematic and multi-institutional study of mCRPC tumors obtained from living affected individuals to determine the landscape of somatic genomic alterations in this cohort, dissect genomic differences between primary prostate cancer and mCRPC, and discover the potential relevance of these findings from a biological and clinical perspective.

RESULTS

Clinical, Biopsy, and Pathology Parameters

An international consortium consisting of eight academic medical center clinical sites was established to capture fresh clinical mCRPC affected individual samples as part of standard-of-care approaches or through a cohort of prospective clinical trials (Figures 1A and 1B). Standard-of-care approaches for mCRPC included abiraterone acetate or enzalutamide. Clinical trials included in this study focused on combination strategies involving abiraterone acetate or enzalutamide, inhibitors of poly ADP ribose polymerase (PARP), or inhibitors of aurora kinase. Here, we report the results of genomic profiling from

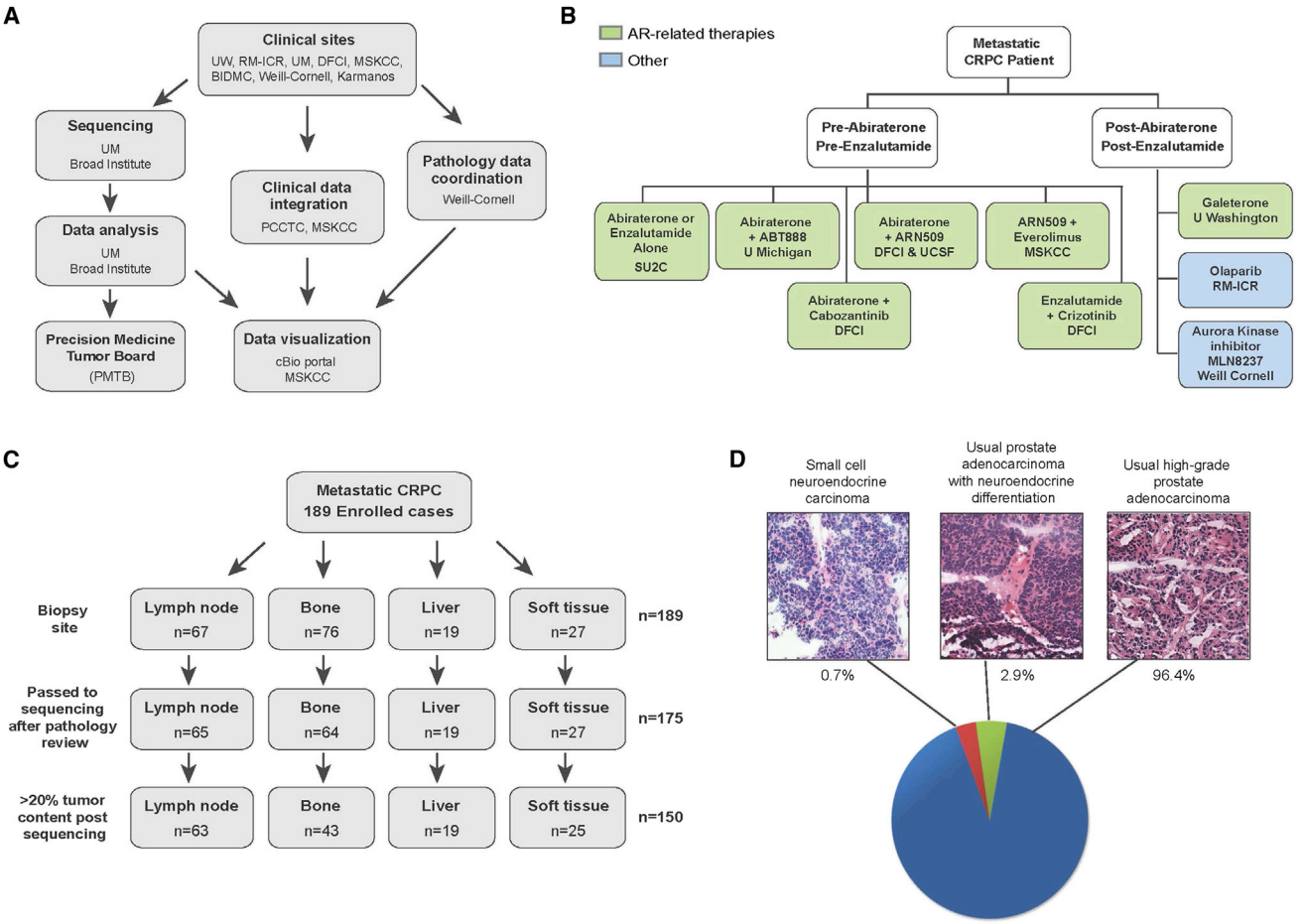

Figure 1. Overview of the SU2C-PCF IDT Multi-Institutional Clinical Sequencing of the mCRPC Project

(A) Schema of multi-institutional clinical sequencing project work flow.

(B) Clinical trials associated with the SU2C-PCF mCRPC project.

(C) Biopsy sites of the samples used for clinical sequencing.

(D) Histopathology of the cohort. Representative images of morphological analysis of mCRPC are shown along with prevalence in our cohort.

mCRPC biopsy samples obtained at time of entry into the cohort study. Future reports will include longitudinal clinical data such as treatment response. The consortium utilized two sequencing and analysis centers, one centralized digital pathology review center, and one centralized data visualization portal (Cerami et al., 2012; Gao et al., 2013; Robinson et al., 2011; Thorvaldsdóttir et al., 2013). Cross-validation of sequencing data from the two original sequencing sites demonstrated comparable variant calls for adequately powered genetic loci (E.M.V.A., D.R., C. Morrissey, C.C.P., S.L. Carter, M. Rosenberg, A. McKenna, A.M.C., L.A.G., and P.S.N., unpublished data).

Here, we describe 150 affected individuals with metastatic disease with complete integrative clinical sequencing results (whole-exome, matched germline, and transcriptome data) (Figure 1C) and summarized in Table S1. 189 affected individuals were enrolled in the study, and 175 cases were sequenced after pathology review and assessment of tumor content. Of these, 150 biopsies had >20% tumor content as defined by computational analysis, based on mutant allele variant fractions and zygosity shifts. The biopsies sequenced were from lymph node (42%), bone (28.7%), liver (12.7%), and other soft tissues (16.7%). Baseline clinical information is available in Table S2. A majority of cases (96.4%) displayed typical high-grade prostate adenocarcinoma features, whereas 2.9% of cases showed neuroendocrine differentiation. One case (0.7%) exhibited small-cell neuroendocrine features (Epstein et al., 2014) (Figure 1D).

Landscape of mCRPC Alterations

Somatic aberrations in a panel of 38 statistically or clinically significant genes are illustrated in Figure 2. Mean target coverage for tumor exomes was 160× and for matched normal exomes was 100×. Although the average mutation rate for mCRPC was 4.4 mutations/Mb, there were four cases that exhibited a mutation rate of nearly 50 per Mb, three of which are likely due to alterations in the mismatch repair genes *MLH1* and *MSH2*, as discussed later.

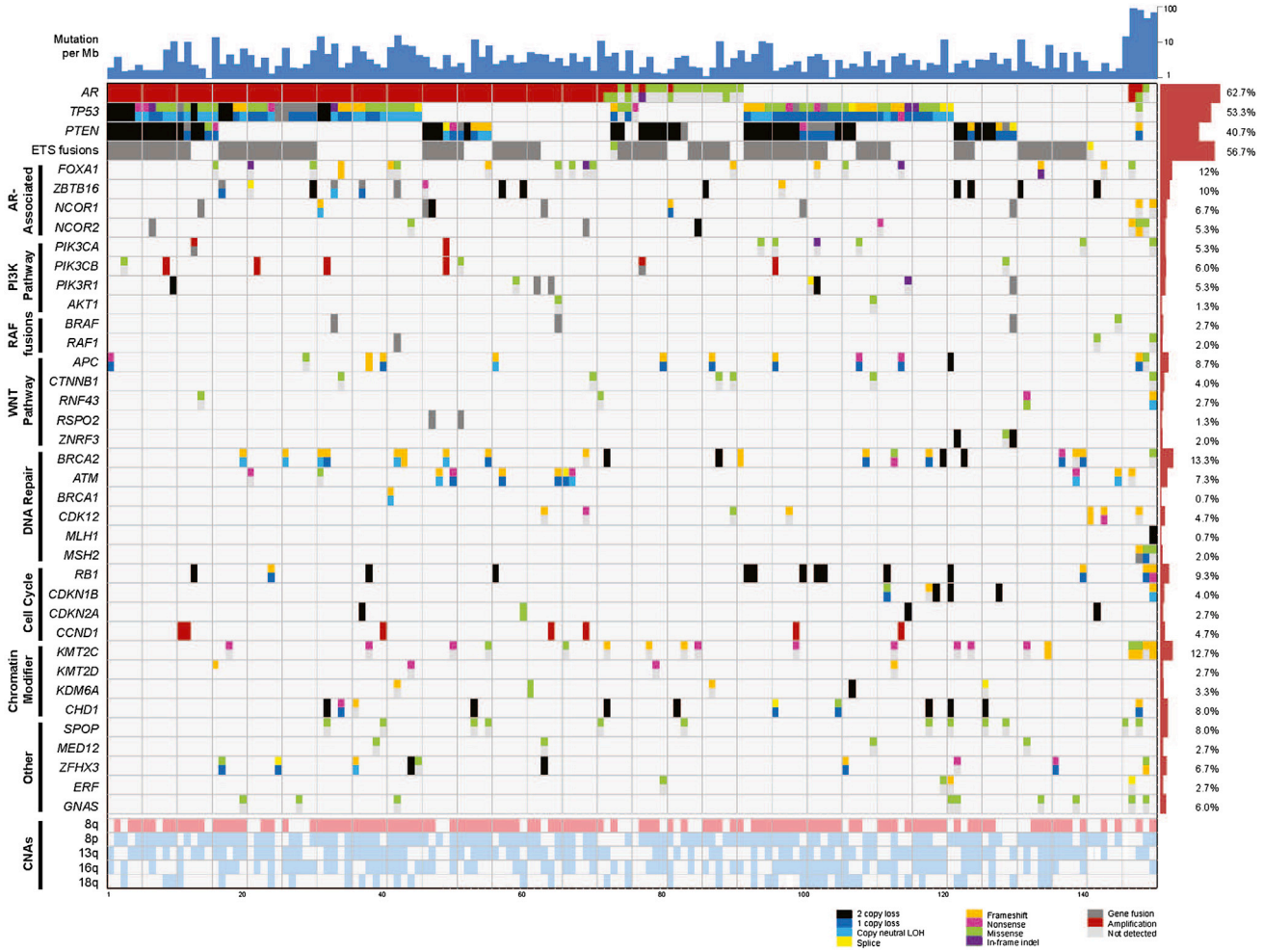

Figure 2. Integrative Landscape Analysis of Somatic and Germline Aberrations in Metastatic CRPC Obtained through DNA and RNA Sequencing of Clinically Obtained Biopsies

Columns represent individual affected individuals, and rows represent specific genes grouped in pathways. Mutations per Mb are shown in the upper histogram, and incidence of aberrations in the cohort is in the right histogram. Copy number variations (CNVs) common to mCRPC are shown in in the lower matrix, with pink representing gain and light blue representing loss. Color legend of the aberrations represented including amplification, two copy loss, one copy loss, copy neutral loss of heterozygosity (LOH), splice site mutation, frameshift mutation, missense mutation, in-frame indel, and gene fusion. Cases with more aberration in a gene are represented by split colors.

Frequent copy number gains of 8q, as well as copy number losses of 8p, 13q, 16q, and 18q, were also observed. The mean number of identified biologically relevant genetic aberrations per case was 7.8 (Figure 2). All mutations identified are presented in Table S3. The landscape of copy number alterations demonstrated expected recurrent amplification peaks (frequent *AR*, 8q gain) and deletion peaks (*CHD1*, *PTEN*, *RB1*, *TP53*) (Figure 3A). Additional frequent focal amplifications were observed in regions encompassing *CCND1* and *PIK3CA* and *PIK3CB*. A new recurrent focal homozygous deletion event was observed in chr11q23, encompassing the transcriptional repressor *ZBTB16*.

To identify gene fusions, analysis of 215 transcriptome libraries derived from the 150 tumor RNAs was performed and identified 4,122 chimeras with at least 4 reads spanning the fusion junction. These fusion junctions resulted from 2,247 gene pairs, an average of 15 gene fusions per tumor (Table S4). Among chimeric fusion transcripts identified, recurrent ETS fusions (Tomlins et al., 2005) were observed in 84 cases (56%), of which the majority were fused to *ERG* and others to *FLI1*, *ETV4*, and *ETV5* (Figure 3B). In addition, potential clinically actionable fusions (involving *BRAF*, *RAF1*, *PIK3CA/B*, or *RSPO2*) were seen in eight cases (Figure S1 and covered subsequently).

To place the mCRPC mutation landscape in the context of primary prostate cancer somatic genomics, we performed a selective enrichment analysis to compare somatic point mutations and short insertion/deletions observed in this cohort with those observed in somatic whole-exome mutation data from 440 primary prostate cancer exomes (Barbieri et al., 2012; The Cancer

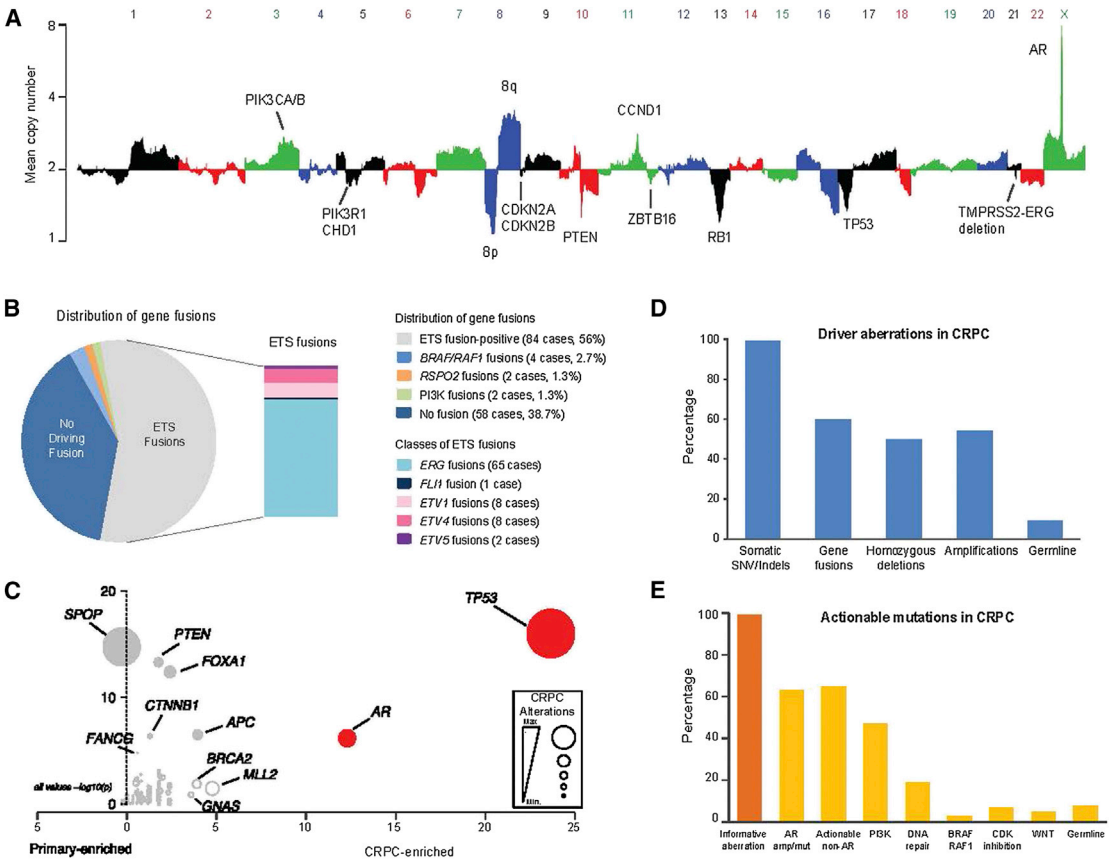

Figure 3. Classes of Genomic Aberrations Seen in mCPRC

(A) Copy number landscape of the SU2C-PCF mCRPC cohort. Individual chromosomes are represented by alternating colors, and key aberrant genes are indicated.

(B) The gene fusion landscape of mCRPC. Pie chart of all driver fusions identified and the box plot represents specific ETS fusions.

(C) Mutations enriched in mCRPC relative to hormone naive primary prostate cancer. Primary prostate cancer data derived from published studies (Barbieri et al., 2012; The Cancer Genome Atlas, 2015). Level of CRPC enrichment is represented by the x axis, and MutSig CRPC significance analysis is provided by the y axis. Diameters are proportional to the number of cases with the specific aberration. Genes of interest are highlighted.

(D) Classes of driver aberrations identified in mCRPC.

(E) Classes of clinically actionable mutations identified in mCRPC.

Genome Atlas, 2015) (Figure 3C and Table S5). Focusing on genes previously implicated in cancer (n = 550), somatic *TP53* mutations were the most selectively mutated ($q < 0.001$; Benjamini-Hochberg), followed by *AR*, *KMT2D*, *APC*, *BRCA2*, and *GNAS* ($q < 0.1$; Benjamini-Hochberg; Table S6). Both *AR* and *GNAS* were mutated exclusively in mCRPC. We found no genes selectively mutated in primary prostate cancer compared to mCRPC.

We identified an established biological "driver" aberration in a cancer-related gene (i.e., known oncogene or tumor suppressor; Table S7) in nearly all the cases (Figure 3D). Although 99% of the mCPRC cases harbored a potential driver single-nucleotide variant (SNV) or indel, other classes of driver aberrations were also highly prevalent. These include driver gene fusions in 60%, driver homozygous deletions in 50% and driver amplifications in 54%. Although informative mutations were present in virtually all mCRPC cases, 63% harbored aberrations in *AR*, an expected finding in castrate-resistant disease but with higher frequency than in prior reports (Figure 3E). Interestingly, even when *AR* was not considered, 65% of cases harbored a putatively clinically actionable alteration (defined as predicting response or resistance to a therapy, having diagnostic or prognostic utility across tumor types) (Table S8) (Roychowdhury et al., 2011; Van Allen et al., 2014c). Non-AR related clinically actionable alterations included aberrations in the PI3K pathway (49%), DNA repair pathway (19%), RAF kinases (3%), CDK inhibitors (7%), and the WNT pathway (5%). In addition to somatic alterations, clinically actionable pathogenic germline variants were seen in 8% of mCRPC affected individuals, potentially emphasizing the need for genetic counseling in affected individuals with prostate cancer.

Genomically Aberrant Pathways in mCRPC

Integrative analysis using both biological and statistical frameworks (Lawrence et al., 2013, 2014) of somatic point mutations,

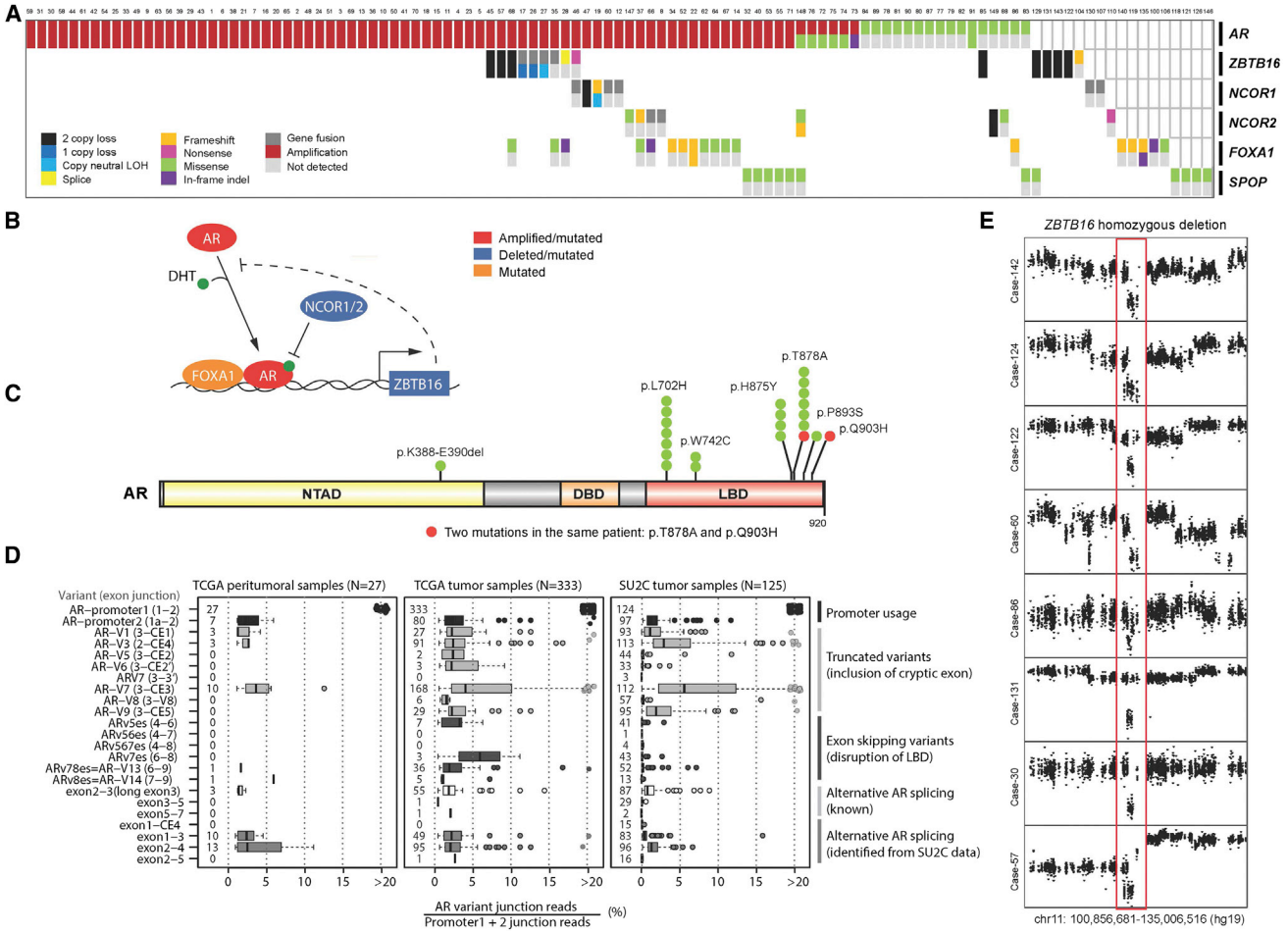

Figure 4. Aberrations in the AR Pathway Found in mCRPC

(A) Cases with aberrations in the AR pathway. Case numbering as in Figure 2.

(B) Key genes found altered in the AR pathway of mCRPC. DHT, dihydrotestosterone.

(C) Point mutations identified in *AR*. Amino acids altered are indicated. NTAD, N-terminal activation. DBD, DNA-binding. LBD, ligand binding.

(D) Splicing landscape of *AR* in mCRPC. Specific splice variants are indicated by exon boundaries, and junction read level is provided. SU2C, this mCRPC cohort. PRAD tumor, primary prostate cancer from the TCGA. PRAD normal, benign prostate from the TCGA.

(E) Homozygous deletion of *ZBTB16*. Copy number plots with x axis representing chromosomal location and the y axis referring to copy number level. Red outline indicates region of *ZBTB16* homozygous loss.

short insertion/deletions, copy number alterations, fusion transcripts, and focused germline variant analysis identified discrete molecular subtypes of mCRPC (Figure 2). These subtypes were classified based on alteration clustering and existing biological pathway knowledge and implicated the *AR* signaling pathway, phosphatidylinositol-4,5-bisphosphate 3-kinase (PI3K), WNT, DNA repair, cell cycle, and chromatin modifier gene sets, among others. The most frequently aberrant genes in mCRPC included *AR* (62.7%), ETS family (56.7%), *TP53* (53.3%), and *PTEN* (40.7%) (Figure 2).

AR Signaling Pathway

In aggregate, 107/150 (71.3%) of cases harbored *AR* pathway aberrations, the majority of which were direct alterations affecting *AR* through amplification and mutation (Figure 4A). Figure 4B summarizes the key genes altered in AR signaling, including *AR* itself, *FOXA1* as a pioneer transcription factor, *NCOR1/2* as negative regulators of AR, *SPOP* as a putative androgen receptor transcriptional regulator (Geng et al., 2013), and *ZBTB16* as an AR inducible target gene that may also negatively regulate *AR*. Recurrent hotspot mutations in *AR* were observed at residues previously reported to confer agonism to AR antagonists such as flutamide (T878A) and bicalutamide (W742C), as well as to glucocorticoids (L702H). Some, but not all, of these affected individuals had documented prior exposures that could explain enrichment for these mutations. Additional clinical data collection is ongoing (Figure 4C). Rare *AR* mutations not previously described were seen in our cohort, although these are of unclear functional significance. Furthermore, one affected individual (Case 89) harbored two putatively

functional *AR* mutations (T878A and Q903H), which may further suggest intra-tumor heterogeneity emerging in the CRPC setting (Carreira et al., 2014). Analysis of *AR* splice variants from RNA-seq data demonstrated a distribution of splice variants observed throughout these mCRPC tumor cases (Figure 4D). Analysis of the TCGA prostate dataset revealed that many of these variants were also present at varying levels in primary prostate cancer and benign prostate tissue. AR-V7, which has been implicated in abiraterone acetate and enzalutamide resistance (Antonarakis et al., 2014), was observed in a majority of pre-abiraterone/enzalutamide cases but at very low ratios relative to full length AR. Implications for treatment response are unknown at this time.

In addition to AR mutations itself, we observed alterations in AR pathway members (Figure 4A). These included known alterations in *NCOR1*, *NCOR2*, and *FOXA1* that have been previously reported in primary prostate cancers and mCRPC (Barbieri et al., 2012; Grasso et al., 2012). In this cohort, truncating and missense mutations in FOXA1 form a cluster near the end of the Forkhead DNA binding domain (Figure S2).

Recurrent homozygous deletions of the androgen-regulated gene *ZBTB16* (also known as PLZF) were seen in 8 (5%) cases (Figure 4E) not previously reported in clinical mCRPC biopsies. Analysis of the minimally deleted region seen in this cohort narrowed the candidate genes in the chr11q23 region to *ZBTB16* (Figure S3). *ZBTB16* has been previously implicated in prostate cancer tumorigenesis and androgen resistance in preclinical models (Cao et al., 2013; Kikugawa et al., 2006), with loss of *ZBTB16* upregulating the MAPK signaling pathway (Hsieh et al., 2015).

New PI3K Pathway Discoveries

The PI3K pathway was also commonly altered, with somatic alterations in 73/150 (49%) of mCRPC affected individuals (Figure 5A). This included biallelic loss of *PTEN*, as well as hotspot mutations, amplifications and activating fusions in *PIK3CA*, and p.E17K activating mutations in *AKT1* (Figure S2). Of note, *PIK3CA* amplifications resulted in overexpression compared to the remaining cohort (Figure S3).

Interestingly, mutations in another member of the PI3K catalytic subunit, *PIK3CB*, were observed in this cohort for the first time, at equivalent positions to canonical activating mutations in PIK3CA (Figure 5B). PIK3CB mutations appeared in the context of PTEN-deficient cases, which is consistent with a previous report demonstrating that some PTEN-deficient cancers are dependent on PIK3CB, rather than PIK3CA (Wee et al., 2008). Furthermore, two affected individuals harbored fusions involving PIK3CA/B, with these events resulting in overexpression of the gene relative to other tumors in the cohort (Figures 5C and 5D).

New Wnt Pathway Discoveries

27/150 (18%) of our cases harbored alterations in the Wnt signaling pathway (Figure 6A). Hotspot activating mutations in *CTNNB1* were seen (Figure 6B), as previously described (Voeller et al., 1998). Notably, recurrent alterations in *APC* were also observed, which have not been previously described in clinical mCRPC affected individuals. This prompted a broader examination of Wnt signaling genes (Figure 6B). Through integrative analysis, we identified alterations in *RNF43* and *ZNRF3*, which were recently described in colorectal, endometrial, and adrenocortical cancers (Assié et al., 2014; Giannakis et al., 2014) and were mutually exclusive with *APC* alterations (Figure 6A). Moreover, we also discovered R-spondin fusions involving *RSPO2*, as previously observed in colorectal carcinoma (Seshagiri et al., 2012) in association with RSPO2 overexpression in these cases (Figure 6C). RSPO2 is a key factor in prostate cancer organoid methodology (Gao et al., 2014). Affected individuals s with aberrations in *RNF43*, *ZNRF3*, or *RSPO2* (overall 6% of affected individuals) are predicted to respond to porcupine inhibitors (Liu et al., 2013).

Cell-Cycle Pathway

We observed *RB1* loss in 21% of cases (Figure S4). Expanding the scope of cell-cycle genes implicated in mCRPC, we noted focal amplifications involving *CCND1* in 9% of cases, as well as less common (< 5%) events in *CDKN2A/B*, *CDKN1B*, and *CDK4* (Figure S4). Cell-cycle derangement, such as through CCND1 amplification or CDKN2A/B loss, may result in enhanced response to CDK4 inhibitors in other tumor types (Finn et al., 2015), and preclinical mCRPC models predict similar activity in prostate cancer (Comstock et al., 2013).

DNA Repair Pathway

Integrative analysis of both the somatic and pathogenic germline alterations in *BRCA2* identified 19/150 (12.7%) of cases with loss of BRCA2, of which ~90% exhibited biallelic loss (Figure 7A). This was commonly a result of somatic point mutation and loss of heterozygosity, as well as homozygous deletion. One of the clinical trials in our consortium is evaluating poly(-ADP-ribose) polymerase (PARP) inhibition in unselected mCRPC affected individuals. Importantly, multiple affected individuals in this trial who experienced clinical benefit harbored biallelic *BRCA2* loss, providing further evidence of clinical actionability (Mateo et al., 2014). Eight affected individuals (5.3%) harbored pathogenic germline *BRCA2* mutations (Figure 7B) with a subsequent somatic event that resulted in biallelic loss, revealing a surprisingly high frequency relative to primary prostate cancer.

We therefore expanded the focus to other DNA repair/recombination genes and identified alterations in at least 34/150 (22.7%) of cases. These include recurrent biallelic loss of *ATM* (Figure 7B), including multiple cases with germline pathogenic alterations. ATM mutations were also observed in affected individuals who achieved clinical responses to PARP inhibition (Mateo et al., 2014). In addition, we noted events in *BRCA1*, *CDK12*, *FANCA*, *RAD51B*, and *RAD51C*. If aberrations of *BRCA2*, *BRCA1*, and *ATM* all confer enhanced sensitivity to PARP inhibitors, 29/150 (19.3%) of mCRPC affected individuals would be predicted to benefit from this therapy. Interestingly, three out of four mCRPC tumors exhibited hypermutation and harbored alterations in the mismatch repair pathway genes *MLH1* or *MSH2* (Figures 2 and 7C), corroborating a recent report identifying structural alterations in *MSH2* and *MSH6* mismatch repair genes in hypermutated prostate cancers (Pritchard et al., 2014).

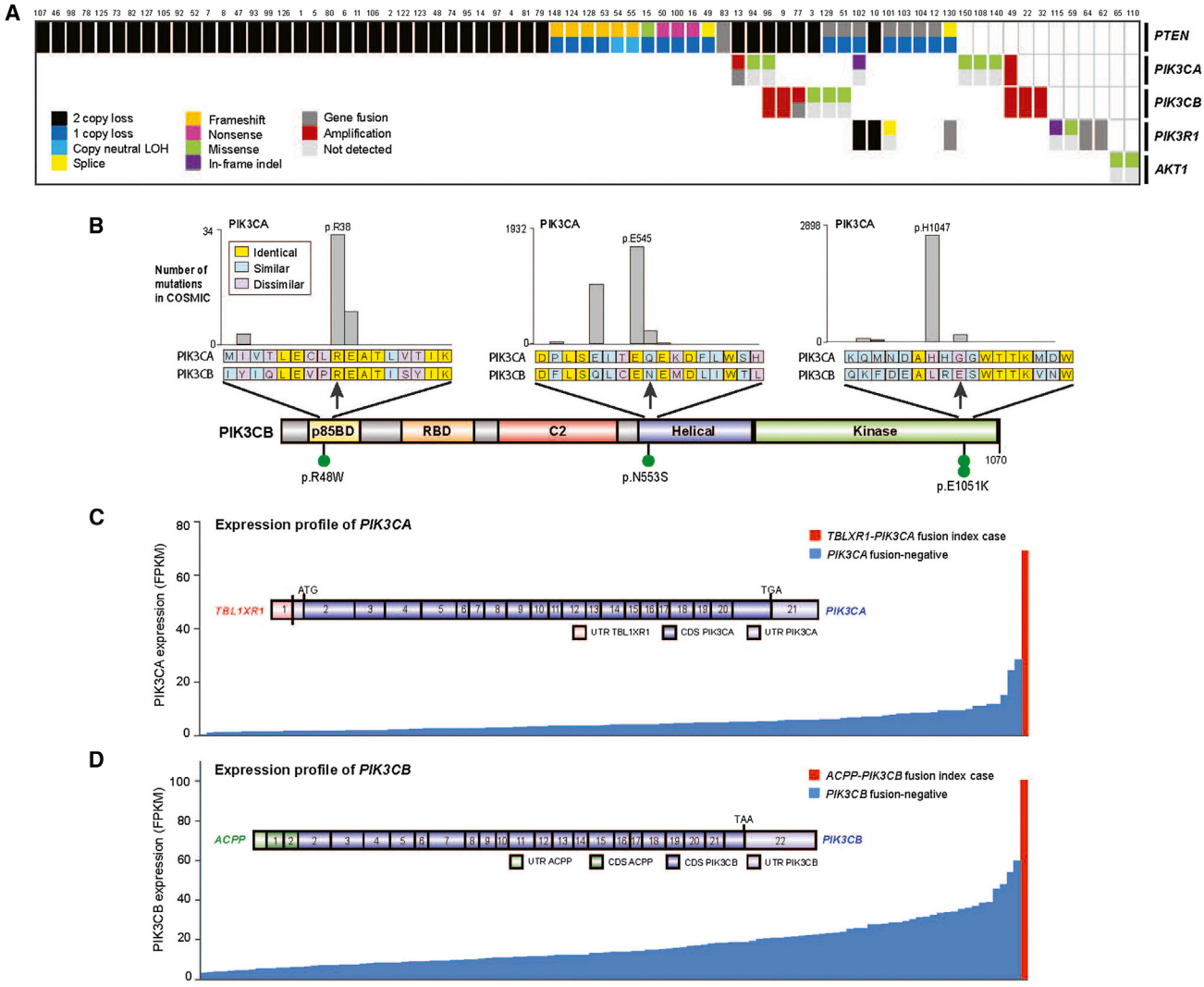

Figure 5. Aberrations in the PI(3)K Pathway Found in mCRPC

(A) Cases with aberrations in the PIK3 pathway. Case numbering as in Figure 2.

(B) Point mutations identified in PIK3CB. Amino acids altered are indicated. Analogous, recurrent COSMIC mutations in PIK3CA are shown as expansion views.

(C) Outlier expression of PK3CA in CRPC case harboring the TBL1XR1-PIK3CA gene fusion. Structure of the gene fusion is inset. UTR, untranslated region. CDS, coding sequence.

(D) As in (C), except for PIK3CB and the ACPP-PIK3CB gene fusion.

DISCUSSION

To effectively implement precision cancer medicine, prospective identification of predictive biomarkers should be performed with information derived from the most contemporary tumor assessments that reflect the affected individual's prior therapies and treatment opportunities. In mCRPC, precision cancer medicine activities have been limited by difficulties obtaining clinical samples from mCRPC affected individuals and a lack of comprehensive genomic data for potentially actionable alterations. By demonstrating the feasibility of prospective genomics in mCRPC and defining the mutational landscape in a focused metastatic clinical cohort, this report may inform multiple genomically driven clinical trials and biological investigations into key mediators of mCRPC. In nearly all of the mCRPC analyzed in this study, we identified biologically informative alterations; almost all harbored at least one driver SNV/indel, and approximately half harbored a driver gene fusion, amplification, or homozygous deletion. Remarkably, in nearly 90% of mCRPC affected individuals, we identified a potentially actionable somatic or germline event.

The high frequency of AR pathway alterations in this cohort strongly implies that the vast majority of mCRPC affected individuals remain dependent on AR signaling for viability. The "second-generation" AR-directed therapies (e.g., abiraterone acetate and enzalutamide) may select for distinct phenotypes that may be indifferent to AR signaling, and prospective

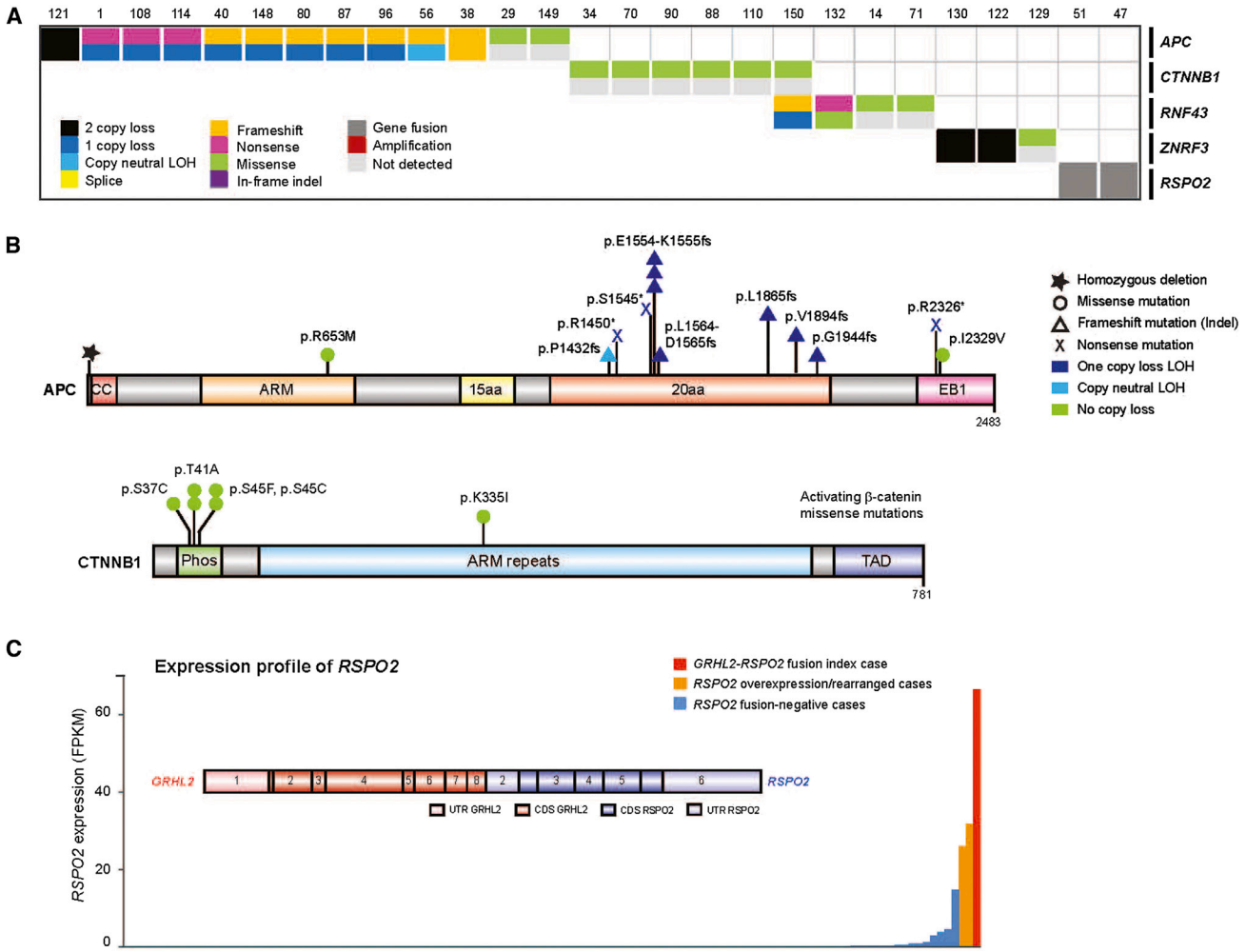

Figure 6. Aberrations in the WNT Pathway Found in mCRPC

(A) Cases with aberrations in the WNT pathway. Case numbering as in Figure 2.

(B) Aberrations identified in APC and CTNNB1. Amino acids altered are indicated. ARM, armadillo repeat. Phos, phosphorylation domain. TAD, *trans*-activating domain. EB1, end binding protein-1 domain. CC, coiled coil.

(C) Outlier expression of *RSPO2* in CRPC and the *GRHL2-RSPO2* gene fusion. RNA-seq expression across our CRPC cohort. Structure of the gene fusion is inset. UTR, untranslated region. CDS, coding sequence.

characterization of such cases will be of particular interest. We hypothesize that affected individuals with acquired *AR* mutations, including new *AR* mutations discovered in this cohort, will harbor differential responses to these second-generation ADT therapies. As the number of affected individuals in this cohort with *AR* mutations increases, we will subsequently be able to link specific AR mutations with clinical phenotypes to determine which mutations confer selective response or resistance to subsequent AR-directed therapy.

Moreover, these data identify multiple therapeutic avenues warranting clinical investigation in the CRPC population. Excluding AR aberrations, 65% of mCRPC have a potentially actionable aberration that may suggest an investigational drug or approved therapy. For example, focusing on the PI3K pathway, PIK3CB-specific inhibitors may have utility in affected individuals with mutation, amplification, and/or fusion of this gene (Schwartz et al., 2015); multiple affected individuals who achieved durable (>1 year) responses to PIK3CB-specificin inhibition harbored activating mutation or amplification in *PIK3CB* (J.S. de Bono et al., 2015, 106th Annual Meeting of the American Association for Cancer Research, abstract). RAF kinase fusions in 3% of mCPRC affected individuals would suggest the use of pan-RAF inhibitors or MEK inhibitors (Palanisamy et al., 2010). In addition, the emergence of porcupine inhibitors (Liu et al., 2013) and R-spondin antibodies may warrant investigation in mCRPC tumors harboring Wnt pathway alterations or specifically R-spondin fusions, respectively. These observations will need to be prospectively assessed in the clinical trials.

Additionally, biallelic inactivation of *BRCA2*, *BRCA1*, or *ATM* was observed in nearly 20% of affected individuals. Previous work in other cancer types suggests that these affected individuals may benefit from PARP inhibitors (Fong et al., 2009;

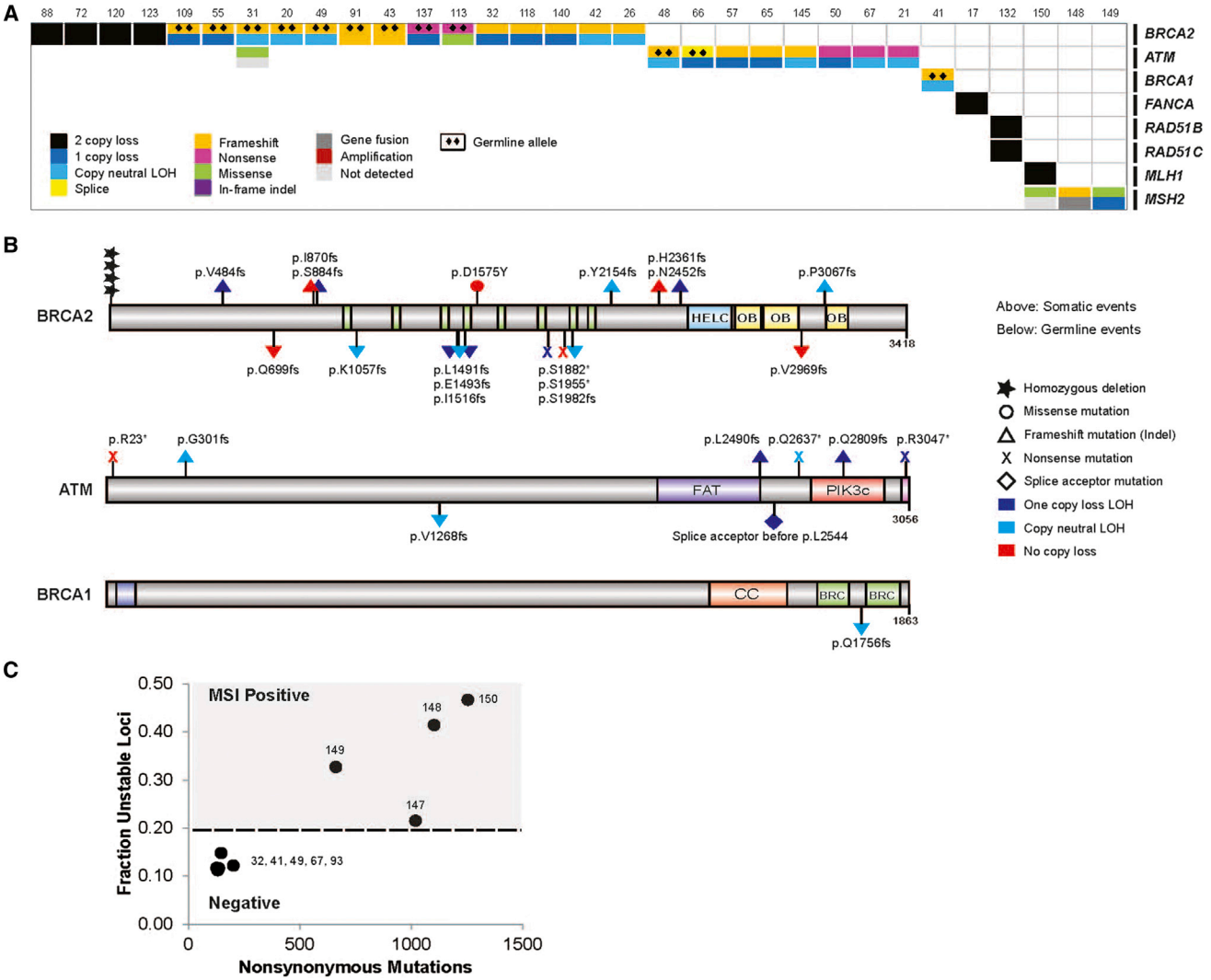

Figure 7. Aberrations in the DNA Repair Pathway Found in mCRPC

(A) Cases with aberrations in the DNA repair pathway. Case numbering as in Figure 2.

(B) Aberrations identified in BRCA2, ATM, and BRCA1. Amino acids altered are indicated. HELC, helical domain. OB, oligonucleotide binding fold. FAT, FRAP-ATM-TRRAP domain. PIK3c, PI3 kinase domain. CC, coiled coil. BRC, Brca repeat.

(C) Microsatellite instability analysis of representative hypermutated CRPC cases and non-hypermutated cases.

Kaufman et al., 2015; Weston et al., 2010) or platinum-based chemotherapy, and prior reports have implicated the presence of germline *BRCA2* alterations in primary prostate cancer with poor survival outcomes (Castro et al., 2013). Given the incidence of pathogenic germline *BRCA2* mutations in this cohort with subsequent somatic events (5%), along with enrichment for somatic *BRCA2* alterations in mCRPC (13%), germline genetic testing in mCRPC affected individuals warrants clinical consideration.

The ability to molecularly characterize mCRPC biopsy samples from affected individuals actively receiving therapy will also enable focused studies of resistance to secondary ADT therapies, including neuroendocrine-like phenotypes. This will require iterative sampling of pre-treatment and resistant tumors from matching affected individuals and may warrant multiregional biopsies from affected individuals (if feasible) given heterogeneity in mCRPC (Carreira et al., 2014; Gundem et al., 2015). Toward that end, in some affected individuals, we observed multiple *AR* mutations emerging in the same biopsy, which may indicate clonal heterogeneity within these mCRPC tumor samples. Additional genomic alterations discovered in this cohort (e.g., *ZBTB16*) warrant exploration in prostate cancer model systems, including organoid cultures (Gao et al., 2014).

Broadly, our effort demonstrates the utility of applying comprehensive genomic principles developed for primary malignancies (e.g., TCGA) to a clinically relevant metastatic tumor cohort. Our effort may also catalyze multi-institutional efforts to profile tumors from cohorts of affected individuals with metastatic, treated tumors in other clinical contexts because our results

demonstrate multiple discoveries within this advanced disease stage that have not been observed in primary tumor profiling. Moreover, this study sets the stage for epigenetic and other profiling efforts in mCRPC not taken in this study, which may enable biological discovery and have immediate therapeutic relevance in mCRPC (Asangani et al., 2014). Overall, our efforts demonstrate the feasibility of comprehensive and integrative genomics on prospective biopsies from individual mCRPC affected individuals to enable precision cancer medicine activities in this large affected individual population.

EXPERIMENTAL PROCEDURES

Affected Individual Enrollment

Affected individuals with clinical evidence of mCRPC who were being considered for abiraterone acetate or enzalutamide as standard of care, or as part of a clinical trial, were considered for enrollment. Affected individuals with metastatic disease accessible by image-guided biopsy were eligible for inclusion. All affected individuals provided written informed consent to obtain fresh tumor biopsies and to perform comprehensive molecular profiling of tumor and germline samples.

Biopsies and Pathology Review

Biopsies of soft tissue or bone metastases were obtained under radiographic guidance. Digital images of biopsy slides were centrally reviewed using schema established to distinguish usual adenocarcinoma from neuroendocrine prostate cancer (Epstein et al., 2014). All images were reviewed by genitourinary oncology pathologists (M.R., J.M.M., L.P.K., S.A.T., R.M., V.R., A.G., M.L., R.L., and M.B.).

Sequencing and Analysis

Normal DNAs from buccal swabs, buffy coats, or whole blood were isolated using the QIAGEN DNeasy Blood & Tissue Kit. Flash-frozen needle biopsies with highest tumor content for each case, as determined by pathology review, were extracted for nucleic acids. Tumor genomic DNA and total RNA were purified from the same sample using the AllPrep DNA/RNA/miRNA kit (QIAGEN) with disruption on a Tissuelyser II (QIAGEN). RNA integrity was verified on an Agilent 2100 Bioanalyzer using RNA Nano reagents (Agilent Technologies).

Whole-exome capture libraries were constructed from 100 ng to 1 μg of DNA from tumor and normal tissue after sample shearing, end repair, and phosphorylation and ligation to barcoded sequencing adaptors. Ligated DNA was size selected for lengths between 200 and 350 bp and subjected to hybrid capture using SureSelect Exome v4 baits (Agilent). Exome sequence data processing and analysis were performed using pipelines at the Broad Institute and the University of Michigan. A BAM file aligned to the hg19 human genome build was produced using Illumina sequencing reads for the tumor and normal sample and the Picard pipeline. Somatic mutation analysis was performed as described previously (Cibulskis et al., 2013; Van Allen et al., 2014c) and reviewed with Integrated Genomics Viewer (IGV) (Robinson et al., 2011).

Copy number aberrations were quantified and reported for each gene as the segmented normalized log2-transformed exon coverage ratios between each tumor sample and matched normal sample (Lonigro et al., 2011). To account for observed associations between coverage ratios and GC content across the genome, lowess normalization was used to correct per-exon coverage ratios prior to segmentation analysis. Mean GC percentage was computed for each targeted region, and a lowess curve was fit to the scatterplot of log2-coverage ratios versus mean GC content across the targeted exome using the lowess function in R (version 2.13.1) with smoothing parameter f = 0.05. The resulting copy ratios were segmented using the circular binary segmentation algorithm (Olshen et al., 2004).

Statistical analysis of recurrently mutated genes was performed using MutSig (Lawrence et al., 2013). Selective enrichment analysis (Van Allen et al., 2014b) of mutations observed in mCRPC compared to primary prostate cancer was performed by tabulating the frequency of affected-individual-normalized mutations observed in either CRPC or primary prostate cancer and performing a two-sided Fisher's exact test using allelic fraction cut off of 0.1 or greater and a set of biologically relevant cancer genes (n = 550 genes) (Futreal et al., 2004). Multiple hypothesis test correction was performed using Benjamini-Hochberg method.

Transcriptome libraries were prepared using 200–1,000 ng of total RNA. PolyA+ RNA isolation, cDNA synthesis, end-repair, A-base addition, and ligation of the Illumina indexed adapters were performed according to the TruSeq RNA protocol (Illumina). Libraries were size selected for 250–300 bp cDNA fragments on a 3% Nusieve 3:1 (Lonza) gel, recovered using QIAEX II reagents (QIAGEN), and PCR amplified using Phusion DNA polymerase (New England Biolabs). Total transcriptome libraries were prepared as above, omitting the poly A selection step and captured using Agilent SureSelect Human All Exon V4 reagents and protocols. Library quality was measured on an Agilent 2100 Bioanalyzer for product size and concentration. Paired-end libraries were sequenced with the Illumina HiSeq 2500, (2×100 nucleotide read length) with sequence coverage to 50 M paired reads and 100 M total reads.

Paired-end transcriptome sequencing reads were aligned to the human reference genome (GRCh37/hg19) using a RNA-seq spliced read mapper Tophat2 (Kim and Salzberg, 2011) (Tophat 2.0.4), with "–fusion-search" option turned on to detect potential gene fusion transcripts. Potential false-positive fusion candidates were filtered out using "Tophat-Post-Fusion" module. Further, the fusion candidates were manually examined for annotation and ligation artifacts. Gene expression, as fragments per kilobase of exon per million fragments mapped (FPKM; normalized measure of gene expression), was calculated using Cufflinks (Trapnell et al., 2012).

ACCESSION NUMBERS

The accession number for the data reported in this paper is dbGap: phs000915.v1.p1.

SUPPLEMENTAL INFORMATION

Supplemental Information includes four figures and eight tables and can be found with this article online at http://dx.doi.org/10.1016/j.cell.2015.05.001.

AUTHOR CONTRIBUTIONS

Y-M.W., N.S., R.J.L., J.-M.M., R.M., M.E.T., C.C.P., G.A., H.B., and W.A. made equal contributions. D.R., E.M.V.A., and R.J.L. coordinated overall sequencing and bioinformatics analysis. Y.M.W., D.R., E.M.V.A., R.J.L., W.A., and J.V. coordinated figures and tables. N.S. developed the SU2C-PCF IDT cBio portal. R.J.L. coordinated copy number analyses. J.-M.M. coordinated central pathology review, and L.P.K coordinated UM pathology analysis. C.C.P. coordinated hypermutation analysis and clinical germline interpretations. R.M., M.E.T, G.A., H.B., M.H., H.I.S., and E.I.H. coordinated clinical enrollment at their specific sites. R.K.B., S.P., and H.D. carried out AR splice variant analysis. J.V. managed the clinical data portal. X.C., J.S., P.F., S.M., and C.S. were involved in project management. R.M., S.A.T., V.E.R., A.G., M.L., S.P.B., R.T.L., M.B., B.D.R., J.-M.M, M.R., and L.D.T. were involved in pathology review. C.B., P.V., J.G., M.G., F.D., O.E., A. Sboner, A. Sigaras, and K.W.E. contributed to bioinformatics analysis. K.A.C., D.C.S., F.Y.F., H.I.S., D.R., S.B.S., M.J.M., R.F., Z.Z., N.T., G.G., J.C.D., J.M., D.M.N., S.T.T., E.Y.Y., Y.C., E.A.M., H.H.C., M.A.S., and K.J.P. are clinical contributors. E.M.V.A., D.R., C.L.S. and A.M.C. wrote the manuscript, which all authors reviewed. P.K., J.S.d.B., M.A.R., P.S.N., and L.A.G. are SU2C-PCF Dream Team Principals, and C.L.S. and A.M.C. are Dream Team co-Leaders.

ACKNOWLEDGMENTS

We thank the affected individuals who participated in this study to better understand the feasibility and utility of precision medicine approaches for advanced prostate cancer. Individuals at our respective institutions who helped with this study are listed by institution. University of Michigan: Karen Giles, Lynda Hodges, Erica Rabban, Ning Yu, Fengyun Su, Rui Wang, Brendan Veeneman, and Moshe Talpaz. MSKCC: Brett Carver, Kristen Curtis, and Julie

Filipenko. DFCI/Broad: Zhenwei Zhang, Daniele Depalo, and Joseph Kramkowski. University of Washington: Jina Taub, Hiep Nguyen, Colm Morrissey, and Robert Vessella. ICR/Royal Marsden: Suzanne Carreira, Ines Figueiredo, and Daniel Nava Rodrigues. This work was supported by a Stand Up To Cancer-Prostate Cancer Foundation Prostate Dream Team Translational Cancer Research Grant. Stand Up To Cancer is a program of the Entertainment Industry Foundation administered by the American Association for Cancer Research (SU2C-AACR-DT0712). The project was also supported by the following NIH awards: Clinical Sequencing Exploratory Research (CSER) UM1HG006508 (A.M.C.), Early Detection Research Network grant UO1 CA111275(A.M.C.), Prostate SPORE grants P50 CA186786 (A.M.C.), P50 CA092629 (H.I.S., C.L.S., and Y.C.), P50 CA90381 (P.K.),and P50 CA097186 (P.S.N., B.M., E.A.M., and L.D.T.), P01 CA163227 (P.S.N., S.P., R.K.B., H.D.), R01 CA116337 (M.A.R., H.B., F.D.), R01 CA155169 (C.L.S.), R01 CA092629, P50 CA092629 (H.I.S., C.L.S., and Y.C.), and R01 CA155169 (C.L.S.). This work was supported by the following DoD awards: W81XWH-09-1-0147 (PCCTC) and DOD PC121341 (H.B.). This work was also supported by the Starr Cancer Consortium (N.S., M.R., C.S., Y.C., L.A.G.). A.M.C. is an A. Alfred Taubman Scholar and an American Cancer Society Professor. H.B. is supported by Damon Runyon Cancer Research Foundation CI-67-13. C.P. is supported by a PCF Young Investigator Award and DoD PC131820. E.M.V. is supported by a NIH 1K08CA188615. E.M.V., N.S., and F.Y.F. are supported by Prostate Cancer Foundation Young Investigator Awards. The RM and ICR team is supported by the Movember Foundation and Prostate Cancer UK, PCF, the ECMC network from Cancer Research UK, the Department of Health in the UK, and BRC grant funding.

Received: March 9, 2015
Revised: April 6, 2015
Accepted: April 27, 2015
Published: May 21, 2015

REFERENCES

American Cancer Society (2015). Cancer Facts and Figures 2015. http://www.cancer.org/acs/groups/content/@editorial/documents/document/acspc-044552.pdf.

Antonarakis, E.S., Lu, C., Wang, H., Luber, B., Nakazawa, M., Roeser, J.C., Chen, Y., Mohammad, T.A., Chen, Y., Fedor, H.L., et al. (2014). AR-V7 and resistance to enzalutamide and abiraterone in prostate cancer. N. Engl. J. Med. *371*, 1028–1038.

Asangani, I.A., Dommeti, V.L., Wang, X., Malik, R., Cieslik, M., Yang, R., Escara-Wilke, J., Wilder-Romans, K., Dhanireddy, S., Engelke, C., et al. (2014). Therapeutic targeting of BET bromodomain proteins in castration-resistant prostate cancer. Nature *510*, 278–282.

Assié, G., Letouzé, E., Fassnacht, M., Jouinot, A., Luscap, W., Barreau, O., Omeiri, H., Rodriguez, S., Perlemoine, K., René-Corail, F., et al. (2014). Integrated genomic characterization of adrenocortical carcinoma. Nat. Genet. *46*, 607–612.

Baca, S.C., Prandi, D., Lawrence, M.S., Mosquera, J.M., Romanel, A., Drier, Y., Park, K., Kitabayashi, N., MacDonald, T.Y., Ghandi, M., et al. (2013). Punctuated evolution of prostate cancer genomes. Cell *153*, 666–677.

Barbieri, C.E., Baca, S.C., Lawrence, M.S., Demichelis, F., Blattner, M., Theurillat, J.P., White, T.A., Stojanov, P., Van Allen, E., Stransky, N., et al. (2012). Exome sequencing identifies recurrent SPOP, FOXA1 and MED12 mutations in prostate cancer. Nat. Genet. *44*, 685–689.

Beer, T.M., Armstrong, A.J., Rathkopf, D.E., Loriot, Y., Sternberg, C.N., Higano, C.S., Iversen, P., Bhattacharya, S., Carles, J., Chowdhury, S., et al.; PREVAIL Investigators (2014). Enzalutamide in metastatic prostate cancer before chemotherapy. N. Engl. J. Med. *371*, 424–433.

Beltran, H., Yelensky, R., Frampton, G.M., Park, K., Downing, S.R., MacDonald, T.Y., Jarosz, M., Lipson, D., Tagawa, S.T., Nanus, D.M., et al. (2013). Targeted next-generation sequencing of advanced prostate cancer identifies potential therapeutic targets and disease heterogeneity. Eur. Urol. *63*, 920–926.

Berger, M.F., Lawrence, M.S., Demichelis, F., Drier, Y., Cibulskis, K., Sivachenko, A.Y., Sboner, A., Esgueva, R., Pflueger, D., Sougnez, C., et al. (2011). The genomic complexity of primary human prostate cancer. Nature *470*, 214–220.

Cao, J., Zhu, S., Zhou, W., Li, J., Liu, C., Xuan, H., Yan, J., Zheng, L., Zhou, L., Yu, J., et al. (2013). PLZF mediates the PTEN/AKT/FOXO3a signaling in suppression of prostate tumorigenesis. PLoS ONE *8*, e77922.

Carreira, S., Romanel, A., Goodall, J., Grist, E., Ferraldeschi, R., Miranda, S., Prandi, D., Lorente, D., Frenel, J.S., Pezaro, C., et al. (2014). Tumor clone dynamics in lethal prostate cancer. Sci. Transl. Med. *6*, 254ra125.

Castro, E., Goh, C., Olmos, D., Saunders, E., Leongamornlert, D., Tymrakiewicz, M., Mahmud, N., Dadaev, T., Govindasami, K., Guy, M., et al. (2013). Germline BRCA mutations are associated with higher risk of nodal involvement, distant metastasis, and poor survival outcomes in prostate cancer. J. Clin. Oncol. *31*, 1748–1757.

Cerami, E., Gao, J., Dogrusoz, U., Gross, B.E., Sumer, S.O., Aksoy, B.A., Jacobsen, A., Byrne, C.J., Heuer, M.L., Larsson, E., et al. (2012). The cBio cancer genomics portal: an open platform for exploring multidimensional cancer genomics data. Cancer Discov. *2*, 401–404.

Cibulskis, K., Lawrence, M.S., Carter, S.L., Sivachenko, A., Jaffe, D., Sougnez, C., Gabriel, S., Meyerson, M., Lander, E.S., and Getz, G. (2013). Sensitive detection of somatic point mutations in impure and heterogeneous cancer samples. Nat. Biotechnol. *31*, 213–219.

Comstock, C.E., Augello, M.A., Goodwin, J.F., de Leeuw, R., Schiewer, M.J., Ostrander, W.F., Jr., Burkhart, R.A., McClendon, A.K., McCue, P.A., Trabulsi, E.J., et al. (2013). Targeting cell cycle and hormone receptor pathways in cancer. Oncogene *32*, 5481–5491.

Cooper, C.S., Eeles, R., Wedge, D.C., Van Loo, P., Gundem, G., Alexandrov, L.B., Kremeyer, B., Butler, A., Lynch, A.G., Camacho, N., et al.; ICGC Prostate Group (2015). Analysis of the genetic phylogeny of multifocal prostate cancer identifies multiple independent clonal expansions in neoplastic and morphologically normal prostate tissue. Nat. Genet. *47*, 367–372.

de Bono, J.S., Logothetis, C.J., Molina, A., Fizazi, K., North, S., Chu, L., Chi, K.N., Jones, R.J., Goodman, O.B., Jr., Saad, F., et al.; COU-AA-301 Investigators (2011). Abiraterone and increased survival in metastatic prostate cancer. N. Engl. J. Med. *364*, 1995–2005.

Epstein, J.I., Amin, M.B., Beltran, H., Lotan, T.L., Mosquera, J.M., Reuter, V.E., Robinson, B.D., Troncoso, P., and Rubin, M.A. (2014). Proposed morphologic classification of prostate cancer with neuroendocrine differentiation. Am. J. Surg. Pathol. *38*, 756–767.

Finn, R.S., Crown, J.P., Lang, I., Boer, K., Bondarenko, I.M., Kulyk, S.O., Ettl, J., Patel, R., Pinter, T., Schmidt, M., et al. (2015). The cyclin-dependent kinase 4/6 inhibitor palbociclib in combination with letrozole versus letrozole alone as first-line treatment of oestrogen receptor-positive, HER2-negative, advanced breast cancer (PALOMA-1/TRIO-18): a randomised phase 2 study. Lancet Oncol. *16*, 25–35.

Fong, P.C., Boss, D.S., Yap, T.A., Tutt, A., Wu, P., Mergui-Roelvink, M., Mortimer, P., Swaisland, H., Lau, A., O'Connor, M.J., et al. (2009). Inhibition of poly(ADP-ribose) polymerase in tumors from BRCA mutation carriers. N. Engl. J. Med. *361*, 123–134.

Futreal, P.A., Coin, L., Marshall, M., Down, T., Hubbard, T., Wooster, R., Rahman, N., and Stratton, M.R. (2004). A census of human cancer genes. Nat. Rev. Cancer *4*, 177–183.

Gao, J., Aksoy, B.A., Dogrusoz, U., Dresdner, G., Gross, B., Sumer, S.O., Sun, Y., Jacobsen, A., Sinha, R., Larsson, E., et al. (2013). Integrative analysis of complex cancer genomics and clinical profiles using the cBioPortal. Sci. Signal. *6*, pl1.

Gao, D., Vela, I., Sboner, A., Iaquinta, P.J., Karthaus, W.R., Gopalan, A., Dowling, C., Wanjala, J.N., Undvall, E.A., Arora, V.K., et al. (2014). Organoid cultures derived from patients with advanced prostate cancer. Cell *159*, 176–187.

Geng, C., He, B., Xu, L., Barbieri, C.E., Eedunuri, V.K., Chew, S.A., Zimmermann, M., Bond, R., Shou, J., Li, C., et al. (2013). Prostate cancer-associated

mutations in speckle-type POZ protein (SPOP) regulate steroid receptor coactivator 3 protein turnover. Proc. Natl. Acad. Sci. USA *110*, 6997–7002.

Giannakis, M., Hodis, E., Jasmine Mu, X., Yamauchi, M., Rosenbluh, J., Cibulskis, K., Saksena, G., Lawrence, M.S., Qian, Z.R., Nishihara, R., et al. (2014). RNF43 is frequently mutated in colorectal and endometrial cancers. Nat. Genet. *46*, 1264–1266.

Grasso, C.S., Wu, Y.M., Robinson, D.R., Cao, X., Dhanasekaran, S.M., Khan, A.P., Quist, M.J., Jing, X., Lonigro, R.J., Brenner, J.C., et al. (2012). The mutational landscape of lethal castration-resistant prostate cancer. Nature *487*, 239–243.

Gundem, G., Van Loo, P., Kremeyer, B., Alexandrov, L.B., Tubio, J.M., Papaemmanuil, E., Brewer, D.S., Kallio, H.M., Högnäs, G., Annala, M., et al.; ICGC Prostate UK Group (2015). The evolutionary history of lethal metastatic prostate cancer. Nature *520*, 353–357.

Hieronymus, H., Schultz, N., Gopalan, A., Carver, B.S., Chang, M.T., Xiao, Y., Heguy, A., Huberman, K., Bernstein, M., Assel, M., et al. (2014). Copy number alteration burden predicts prostate cancer relapse. Proc. Natl. Acad. Sci. USA *111*, 11139–11144.

Hong, M.K., Macintyre, G., Wedge, D.C., Van Loo, P., Patel, K., Lunke, S., Alexandrov, L.B., Sloggett, C., Cmero, M., Marass, F., et al. (2015). Tracking the origins and drivers of subclonal metastatic expansion in prostate cancer. Nat. Commun. *6*, 6605.

Hsieh, C.L., Botta, G., Gao, S., Li, T., Van Allen, E.M., Treacy, D.J., Cai, C., He, H.H., Sweeney, C.J., Brown, M., et al. (2015). PLZF, a tumor suppressor genetically lost in metastatic castration-resistant prostate cancer, is a mediator of resistance to androgen deprivation therapy. Cancer Res. Published online March 25, 2015. http://dx.doi.org/10.1158/0008-5472.CAN-14-3602.

Kaufman, B., Shapira-Frommer, R., Schmutzler, R.K., Audeh, M.W., Friedlander, M., Balmaña, J., Mitchell, G., Fried, G., Stemmer, S.M., Hubert, A., et al. (2015). Olaparib monotherapy in patients with advanced cancer and a germline BRCA1/2 mutation. J. Clin. Oncol. *33*, 244–250.

Kikugawa, T., Kinugasa, Y., Shiraishi, K., Nanba, D., Nakashiro, K., Tanji, N., Yokoyama, M., and Higashiyama, S. (2006). PLZF regulates Pbx1 transcription and Pbx1-HoxC8 complex leads to androgen-independent prostate cancer proliferation. Prostate *66*, 1092–1099.

Kim, D., and Salzberg, S.L. (2011). TopHat-Fusion: an algorithm for discovery of novel fusion transcripts. Genome Biol. *12*, R72.

Lalonde, E., Ishkanian, A.S., Sykes, J., Fraser, M., Ross-Adams, H., Erho, N., Dunning, M.J., Halim, S., Lamb, A.D., Moon, N.C., et al. (2014). Tumour genomic and microenvironmental heterogeneity for integrated prediction of 5-year biochemical recurrence of prostate cancer: a retrospective cohort study. Lancet Oncol. *15*, 1521–1532.

Lawrence, M.S., Stojanov, P., Polak, P., Kryukov, G.V., Cibulskis, K., Sivachenko, A., Carter, S.L., Stewart, C., Mermel, C.H., Roberts, S.A., et al. (2013). Mutational heterogeneity in cancer and the search for new cancer-associated genes. Nature *499*, 214–218.

Lawrence, M.S., Stojanov, P., Mermel, C.H., Robinson, J.T., Garraway, L.A., Golub, T.R., Meyerson, M., Gabriel, S.B., Lander, E.S., and Getz, G. (2014). Discovery and saturation analysis of cancer genes across 21 tumour types. Nature *505*, 495–501.

Liu, J., Pan, S., Hsieh, M.H., Ng, N., Sun, F., Wang, T., Kasibhatla, S., Schuller, A.G., Li, A.G., Cheng, D., et al. (2013). Targeting Wnt-driven cancer through the inhibition of Porcupine by LGK974. Proc. Natl. Acad. Sci. USA *110*, 20224–20229.

Lonigro, R.J., Grasso, C.S., Robinson, D.R., Jing, X., Wu, Y.M., Cao, X., Quist, M.J., Tomlins, S.A., Pienta, K.J., and Chinnaiyan, A.M. (2011). Detection of somatic copy number alterations in cancer using targeted exome capture sequencing. Neoplasia *13*, 1019–1025.

Mateo, J., Hall, E., Sandhu, S., Omlin, A., Miranda, S., Carreira, S., Goodall, J., Gillman, A., Mossop, H., Ralph, C., et al. (2014). Antitumour activity of the PARP inhibitor olaparib in unselected sporadic castration-resistant prostate cancer (CRPC) in the TOPARP trial. Annals Oncol. *25*, 1–41.

Mehra, R., Kumar-Sinha, C., Shankar, S., Lonigro, R.J., Jing, X., Philips, N.E., Siddiqui, J., Han, B., Cao, X., Smith, D.C., et al. (2011). Characterization of bone metastases from rapid autopsies of prostate cancer patients. Clin. Cancer Res. *17*, 3924–3932.

Olshen, A.B., Venkatraman, E.S., Lucito, R., and Wigler, M. (2004). Circular binary segmentation for the analysis of array-based DNA copy number data. Biostatistics *5*, 557–572.

Palanisamy, N., Ateeq, B., Kalyana-Sundaram, S., Pflueger, D., Ramnarayanan, K., Shankar, S., Han, B., Cao, Q., Cao, X., Suleman, K., et al. (2010). Rearrangements of the RAF kinase pathway in prostate cancer, gastric cancer and melanoma. Nat. Med. *16*, 793–798.

Pflueger, D., Terry, S., Sboner, A., Habegger, L., Esgueva, R., Lin, P.C., Svensson, M.A., Kitabayashi, N., Moss, B.J., MacDonald, T.Y., et al. (2011). Discovery of non-ETS gene fusions in human prostate cancer using next-generation RNA sequencing. Genome Res. *21*, 56–67.

Pritchard, C.C., Morrissey, C., Kumar, A., Zhang, X., Smith, C., Coleman, I., Salipante, S.J., Milbank, J., Yu, M., Grady, W.M., et al. (2014). Complex MSH2 and MSH6 mutations in hypermutated microsatellite unstable advanced prostate cancer. Nat. Commun. *5*, 4988.

Robinson, J.T., Thorvaldsdóttir, H., Winckler, W., Guttman, M., Lander, E.S., Getz, G., and Mesirov, J.P. (2011). Integrative genomics viewer. Nat. Biotechnol. *29*, 24–26.

Roychowdhury, S., Iyer, M.K., Robinson, D.R., Lonigro, R.J., Wu, Y.M., Cao, X., Kalyana-Sundaram, S., Sam, L., Balbin, O.A., Quist, M.J., et al. (2011). Personalized oncology through integrative high-throughput sequencing: a pilot study. Sci. Transl. Med. *3*, 111ra121.

Ryan, C.J., Smith, M.R., de Bono, J.S., Molina, A., Logothetis, C.J., de Souza, P., Fizazi, K., Mainwaring, P., Piulats, J.M., Ng, S., et al.; COU-AA-302 Investigators (2013). Abiraterone in metastatic prostate cancer without previous chemotherapy. N. Engl. J. Med. *368*, 138–148.

Scher, H.I., Fizazi, K., Saad, F., Taplin, M.E., Sternberg, C.N., Miller, K., de Wit, R., Mulders, P., Chi, K.N., Shore, N.D., et al.; AFFIRM Investigators (2012). Increased survival with enzalutamide in prostate cancer after chemotherapy. N. Engl. J. Med. *367*, 1187–1197.

Schwartz, S., Wongvipat, J., Trigwell, C.B., Hancox, U., Carver, B.S., Rodrik-Outmezguine, V., Will, M., Yellen, P., de Stanchina, E., Baselga, J., et al. (2015). Feedback suppression of PI3Kα signaling in PTEN-mutated tumors is relieved by selective inhibition of PI3Kβ. Cancer Cell *27*, 109–122.

Seshagiri, S., Stawiski, E.W., Durinck, S., Modrusan, Z., Storm, E.E., Conboy, C.B., Chaudhuri, S., Guan, Y., Janakiraman, V., Jaiswal, B.S., et al. (2012). Recurrent R-spondin fusions in colon cancer. Nature *488*, 660–664.

Taplin, M.E., Bubley, G.J., Shuster, T.D., Frantz, M.E., Spooner, A.E., Ogata, G.K., Keer, H.N., and Balk, S.P. (1995). Mutation of the androgen-receptor gene in metastatic androgen-independent prostate cancer. N. Engl. J. Med. *332*, 1393–1398.

Taylor, B.S., Schultz, N., Hieronymus, H., Gopalan, A., Xiao, Y., Carver, B.S., Arora, V.K., Kaushik, P., Cerami, E., Reva, B., et al. (2010). Integrative genomic profiling of human prostate cancer. Cancer Cell *18*, 11–22.

The Cancer Genome Atlas. (2015). The molecular taxonomy of primary prostate cancer. http://www.cbioportal.org/study.do?cancer_study_id=prad_tcga_pub.

Thorvaldsdóttir, H., Robinson, J.T., and Mesirov, J.P. (2013). Integrative Genomics Viewer (IGV): high-performance genomics data visualization and exploration. Brief. Bioinform. *14*, 178–192.

Tomlins, S.A., Rhodes, D.R., Perner, S., Dhanasekaran, S.M., Mehra, R., Sun, X.W., Varambally, S., Cao, X., Tchinda, J., Kuefer, R., et al. (2005). Recurrent fusion of TMPRSS2 and ETS transcription factor genes in prostate cancer. Science *310*, 644–648.

Tomlins, S.A., Laxman, B., Dhanasekaran, S.M., Helgeson, B.E., Cao, X., Morris, D.S., Menon, A., Jing, X., Cao, Q., Han, B., et al. (2007). Distinct classes of chromosomal rearrangements create oncogenic ETS gene fusions in prostate cancer. Nature *448*, 595–599.

Trapnell, C., Roberts, A., Goff, L., Pertea, G., Kim, D., Kelley, D.R., Pimentel, H., Salzberg, S.L., Rinn, J.L., and Pachter, L. (2012). Differential gene and

transcript expression analysis of RNA-seq experiments with TopHat and Cufflinks. Nat. Protoc. *7*, 562–578.

Van Allen, E.M., Foye, A., Wagle, N., Kim, W., Carter, S.L., McKenna, A., Simko, J.P., Garraway, L.A., and Febbo, P.G. (2014a). Successful whole-exome sequencing from a prostate cancer bone metastasis biopsy. Prostate Cancer Prostatic Dis. *17*, 23–27.

Van Allen, E.M., Mouw, K.W., Kim, P., Iyer, G., Wagle, N., Al-Ahmadie, H., Zhu, C., Ostrovnaya, I., Kryukov, G.V., O'Connor, K.W., et al. (2014b). Somatic ERCC2 mutations correlate with cisplatin sensitivity in muscle-invasive urothelial carcinoma. Cancer Discov. *4*, 1140–1153.

Van Allen, E.M., Wagle, N., Stojanov, P., Perrin, D.L., Cibulskis, K., Marlow, S., Jane-Valbuena, J., Friedrich, D.C., Kryukov, G., Carter, S.L., et al. (2014c). Whole-exome sequencing and clinical interpretation of formalin-fixed, paraffin-embedded tumor samples to guide precision cancer medicine. Nat. Med. *20*, 682–688.

Voeller, H.J., Truica, C.I., and Gelmann, E.P. (1998). Beta-catenin mutations in human prostate cancer. Cancer Res. *58*, 2520–2523.

Wang, X.S., Shankar, S., Dhanasekaran, S.M., Ateeq, B., Sasaki, A.T., Jing, X., Robinson, D., Cao, Q., Prensner, J.R., Yocum, A.K., et al. (2011). Characterization of KRAS rearrangements in metastatic prostate cancer. Cancer Discov. *1*, 35–43.

Wee, S., Wiederschain, D., Maira, S.M., Loo, A., Miller, C., deBeaumont, R., Stegmeier, F., Yao, Y.M., and Lengauer, C. (2008). PTEN-deficient cancers depend on PIK3CB. Proc. Natl. Acad. Sci. USA *105*, 13057–13062.

Weston, V.J., Oldreive, C.E., Skowronska, A., Oscier, D.G., Pratt, G., Dyer, M.J., Smith, G., Powell, J.E., Rudzki, Z., Kearns, P., et al. (2010). The PARP inhibitor olaparib induces significant killing of ATM-deficient lymphoid tumor cells in vitro and in vivo. Blood *116*, 4578–4587.